DESIGN AND PERFORMANCE OF A RING DYE LASER

by

MARTIN CHRISTIAN FISCHER

THESIS

Presented to the Faculty of the Graduate School of

The University of Texas at Austin

in Partial Fulfillment

of the Requirements

for the Degree of

MASTER OF ARTS

THE UNIVERSITY OF TEXAS AT AUSTIN

December, 1993

DESIGN AND PERFORMANCE OF A RING DYE LASER

APPROVED BY

SUPERVISORY COMMITTEE:

Supervisor: _____

Mark G. Raizen

_____

Lothar W. Frommhold

Für meine Familie und all meine Freunde

Acknowledgments

I would like to thank Professor Mark Raizen for the help, guidance and confidence he has given me while supervising my graduate work. I am indebted to Dr. Fred Moore for the advice and many ideas he has given me. Also I would like to thank my fellow students Cyrus Bharucha, Luke Graham, Pat Morrow and John Robinson for many discussions and the help they provided me. My thanks also go to my friend Michael Käsbauer who helped me with the design and assembly of the laser.

I would like to thank Professor Lothar Frommhold and Professor Manfred Fink for advising me during my stay at the University of Texas.

I would like to thank Dr. Jim Bergquist for providing preliminary drawings of his laser and a great deal of technical advice.

To my family and friends go my sincerest thanks for making this work possible by giving me love and support throughout this time.

Martin Christian Fischer

The University of Texas at Austin

December, 1993

ABSTRACT

DESIGN AND PERFORMANCE OF A RING DYE LASER

by

MARTIN CHRISTIAN FISCHER, M.A.

The University of Texas at Austin, 1993

SUPERVISOR: Mark G. Raizen

This thesis describes the design and performance of a ring dye laser. This cw-laser is tunable and runs single mode. A birefringent filter, a thin and a thick etalon serve as mode selective elements. An optical diode forces the laser to run unidirectional. As an active medium Rhodamine 6G dissolved in ethylene glycol is used. The laser frequency is locked to an external reference cavity using the Hänsch-Couillaud scheme.

The linewidth, output power and wavelength tunability have been measured and are discussed here.

Table of Contents

List of Tables

List of Figures

Chapter 1

Introduction

This Master's project was to design and build a ring dye laser, which is to be used in two different experiments in the Quantum Optics Laboratory of Dr. Mark Raizen.

The first experiment is an investigation of quantum dynamical localization of atomic beam deflection by a standing light wave [1]. A cold neutral atomic beam is sent through a modulated standing light wave and is deflected by diffusive momentum transfer by the field. According to a classical description one should observe chaotic behavior for increasing modulation. But due to quantum effects, dynamical localization is predicted theoretically.

The second experiment uses cold atomic beams to probe states of small photon number in an optical cavity. This research may enable quantum non-demolition measurements of the field [2].

Chapter 2

Operation Requirements

The first experiment described above requires two laser beams with different wavelengths around the resonant frequency of the atoms, which in this case is the sodium D_2 line at 589 nm. One of the beams is to be detuned from this resonant frequency by up to tens of GHz. This means that these frequencies are too far apart to be generated by electro-optical or acousto-optical modulation of a single laser beam. Since there is only one tunable laser available in the laboratory, this experiment cannot be run without an additional laser.

The second experiment uses a beryllium line at 313 nm as the resonant frequency. This UV-light is generated by frequency doubling of red light with a wavelength of 626 nm.

To be usable in both experiments, the laser must be tunable and include both frequencies in the tuning range. The setup for the experiments also requires the laser to run single mode. The laser has to be stable in frequency without locking to an atomic transition, though it should be possible to set up this locking scheme if necessary.

There is also only one argon-ion-laser available in the laboratory, which simultaneously has to pump a commercial dye laser and the dye laser designed. This limits the available pump power to 2–3 W.

Chapter 3

Operation Principles and Design

3.1 Dye Laser Principles

A common system to meet the above requirements for the beam is a dye laser. The active media are organic dye molecules dissolved in liquid. When excited by visible or UV light they show a broad-band fluorescence spectrum. This can be explained with the diagram in Figure 3.1:

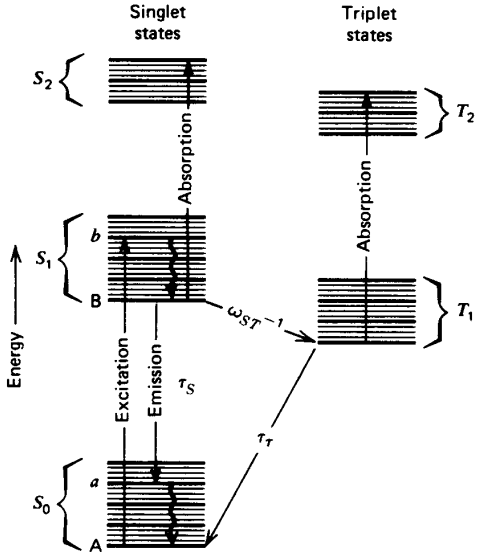

Figure 3.1: Energy levels of a dye molecule

The heavy horizontal lines represent vibrational states, the lighter lines represent the rotational fine structure [3].

When the dye solution is irradiated by the pump light, dye molecules are pumped from the rovibronic levels of the ground state S_0 to higher rovibronic levels of the excited singlet state S_1. This is followed by a fast radiationless transition to the lowest level of the S_1 state, induced by collisions with the solvent. This state is depopulated either by decay into different levels of the ground state S_0 or by radiationless transition into the triplet state T_1. The transition into the ground state S_0 determines the frequency of the laser. Since the rovibronic levels of the dye molecules are strongly collision-broadened by interaction with the solvent, the fluorescence spectra of the dye molecule are continuous rather than discrete. This broadening gives the laser continuous tunability over a wide range of frequencies.

The transition from S_1 into the long-living triplet state T_1 not only decreases the number of molecules available for building up population inversion between S_0 and S_1, but also allows absorption of the laser radiation by transition from T_1 into higher triplet states. To minimize this effect the molecules with populated state T_1 should be removed from the active zone in a time scale much shorter than the life-time of T_1. This is done by forming a flat stream of dye solution in a nozzle and inserting this free jet at this point in the cavity, where the path inside the cavity and the focused pump beam overlap. At high enough pressure, the time of flight of the dye through the active region satisfies the condition above.

There are various dyes available commercially. To obtain the tuning range necessary for the two experiments described above, Rhodamine 6G (R6G) dissolved in ethylene glycol has been chosen (Figure 3.2).

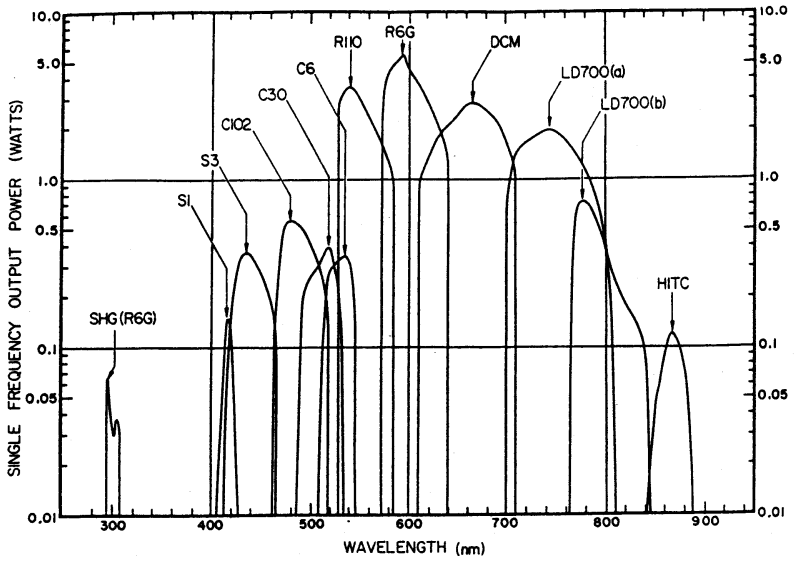

Figure 3.2: Various dye tuning curves

Single-frequency tuning curves obtained with the CR-699-21 dye laser for different pump powers [4].

3.2 Design of the Cavity

In a linear laser cavity the spatial hole burning effect [5] can occur and impede single mode operation. It can also induce power losses due to the fact that the molecules in the active region that are in the nodes of the standing wave cannot contribute to the laser gain. To avoid this complication, the geometry of a ring laser is used (Figure 3.3).

In principle, the opening angles of the cavity are chosen as small as possible to reduce the effect of astigmatism and coma. The compensation for astigmatism and coma induced by the optical elements in the cavity — by the optical diode, the birefringent filter and the dye jet — can be achieved by

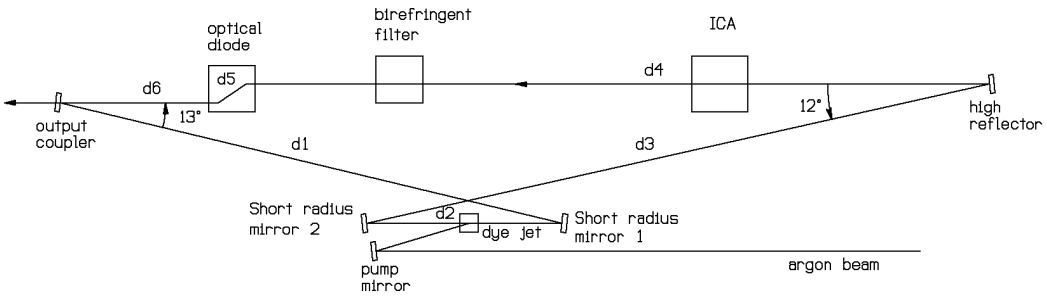

Figure 3.3: Geometry of the laser

choosing the opening angles in a way that those aberration effects are compensated by the aberrations induced by the curved mirrors. The opening angles of 12° and 13° were obtained from the available preliminary design. These angles also provide enough space to place all necessary elements in the ring.

The total optical pathlength L in the ring cavity determines the free spectral range $\delta\nu$ according to

$$\delta\nu = \frac{1}{\tau} = \frac{c}{L} \tag{3.1}$$

On the one hand, for single mode operation it is favorable to choose $\delta\nu$ as large as possible, on the other hand the path length L must be long enough to fit all optical elements in the cavity. The optical pathlength of $L = 1.5$ m was chosen, which corresponds to a free spectral range of $\delta\nu = 200$ MHz.

To obtain an output beam with reasonable parameters the cavity has to be stable and the spot sizes in the cavity have to be optimized. To calculate the beam inside the cavity the $ABCD$ matrix analysis [6] was used.

For the simulation of the beam inside the cavity the output coupler was chosen as the starting point of the calculation. The diagonal distances $d1$ and $d3$ are set by the distance of the parallel beams and the opening angles and are treated as constants. The length $d6$ could be arbitrarily chosen and $d5$ accounts for the path inside the optical diode. The values for $d2$ and $d4$ were to be optimized. Considering the total path length L as constant, this is equivalent to the optimization of the distance between the output coupler (OC) and the high reflector (HR). The following types of mirrors were used (Table 3.1, SR are short radius mirrors):

mirror	OC	HR	SR1	SR2
radius of curvature	∞	30cm	10cm	10cm
diameter	0.5”	0.5”	7.75mm	7.75mm
reflectivity	95%	>99.99%	>99.99%	>99.99%

Table 3.1: Mirrors used

The first step was to determine the distances within the cavity to obtain stable resonator modes. This was done by multiplying successively all transfer matrices and analyzing the final matrix. Requiring the cavity mode to reproduce itself in one round trip, we get the following stability condition for the final $ABCD$ matrix [6]:

$$-1 < \cos\Theta = \frac{1}{2}\,\mathrm{trace}\begin{pmatrix} A & B \\ C & D \end{pmatrix} < 1 \tag{3.2}$$

Figure 3.4 shows $\cos\Theta$ as a function of the distance l between the output coupler (OC) and the high reflector (HR). Stable resonator modes are therefore only possible when l lies between 61.5 cm and 62.6 cm.

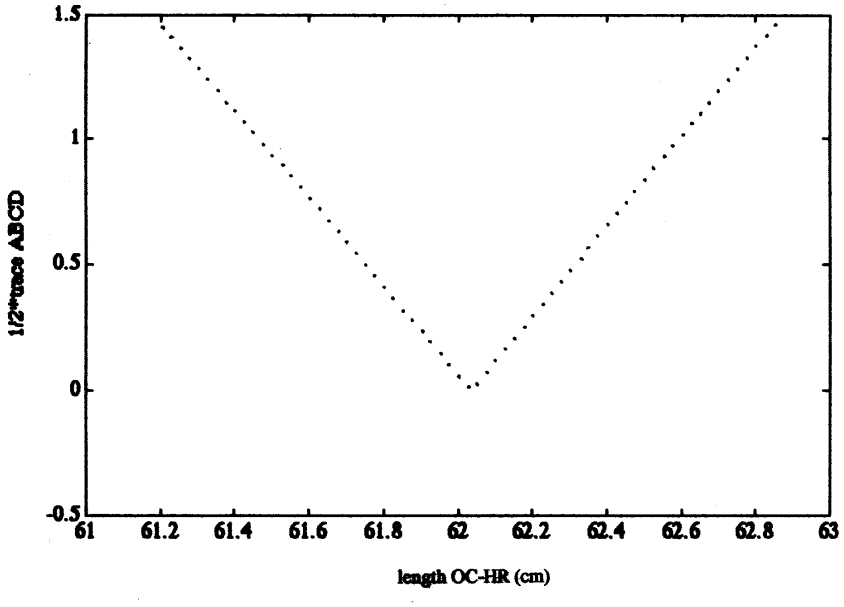

Figure 3.4: Stability condition for the cavity

The spot size ω of a cavity is related to the beam parameter q by

$$\omega = \sqrt{\frac{\lambda}{\pi \left| \mathrm{Im}\left(\frac{1}{q}\right) \right|}} \tag{3.3}$$

where the beam parameter q changes to

$$q_2 = \frac{Aq_1 + B}{Cq_1 + D} \tag{3.4}$$

after passing through an element with the corresponding $ABCD$ matrix. From the condition that the beam parameter reproduces itself after one round trip in the cavity

$$q_{final} = \frac{Aq_{initial} + B}{Cq_{initial} + D} = q_{initial} \tag{3.5}$$

the starting parameter $q_{initial}$ at the output coupler can be obtained as a solution of above quadratic equation where the $ABCD$ matrix describes the transfer

matrix of the whole cavity. To calculate the spot size throughout the cavity, $q_{initial}$ is multiplied by step-$ABCD$ matrices or the transfer matrix of an optical element respectively and the spot size is obtained by Equation 3.3.

It is critical that the focused pump beam and the beam waist inside the cavity coincide at the point where both cross the active medium and both spot sizes have to be approximately equal. Spot sizes of the pump beam which are too small result in substantial power losses, whereas spot sizes which are too big may allow higher order resonator modes to reach the gain threshold. To check this condition the size of the beam waist between the two short radius mirrors are plotted as a function of l (Figure 3.5).

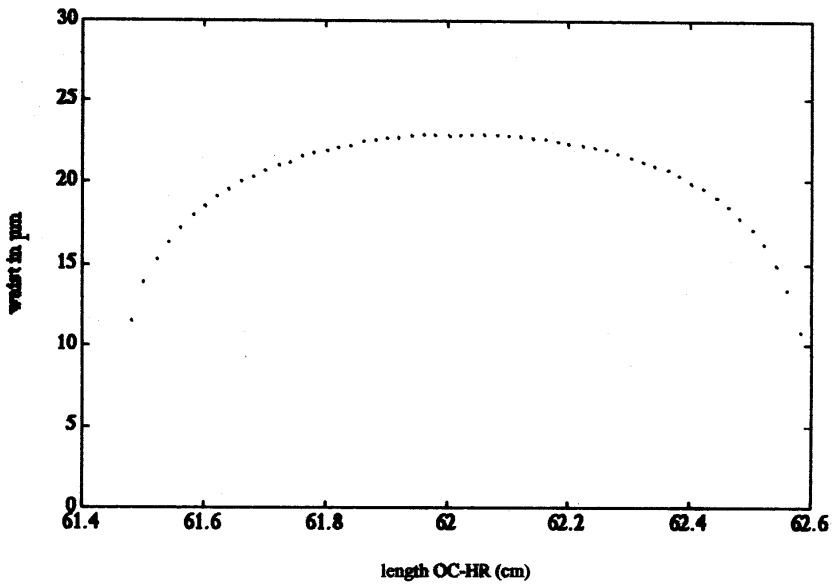

Figure 3.5: Waist between SR1 and SR2

The length l was then chosen centered on the plateau in Figure 3.5

at position $l = 62.0$ cm not to have too sensitive a setup. The beam waist of approximately 23 μm between SR1 and SR2 is comparable to the focused argon ion pump beam. The calculated waist size of the pump beam at its focal point is 5 μm and the spot size at the jet can easily be adjusted to the waist size of the cavity by moving the focus of the pump mirror.

The choice of l determines the distances $d1$–$d6$ to be (Table 3.2):

d_1	d_2	d_3	d_4	d_5	d_6
35.23cm	11.85cm	40.32cm	50.80cm	1.20cm	10.00cm

Table 3.2: Optimized distances in the cavity

With these distances the spot size throughout the cavity is plotted versus the position in the cavity, starting at the output coupler along the paths $d1$–$d6$ (Figure 3.6).

With a beam waist ω_0 of about 230 μm next to the output coupler and a wavelength of 589 nm, the beam divergence Θ (half-apex angle) of the output beam can be determined by [3]

$$\Theta \approx \left(\frac{\lambda}{\pi \omega_0} \right) \tag{3.6}$$

to be $\theta \approx 0.8$ mrad. Since the output coupler is flat it does not change the angle of divergence of the beam.

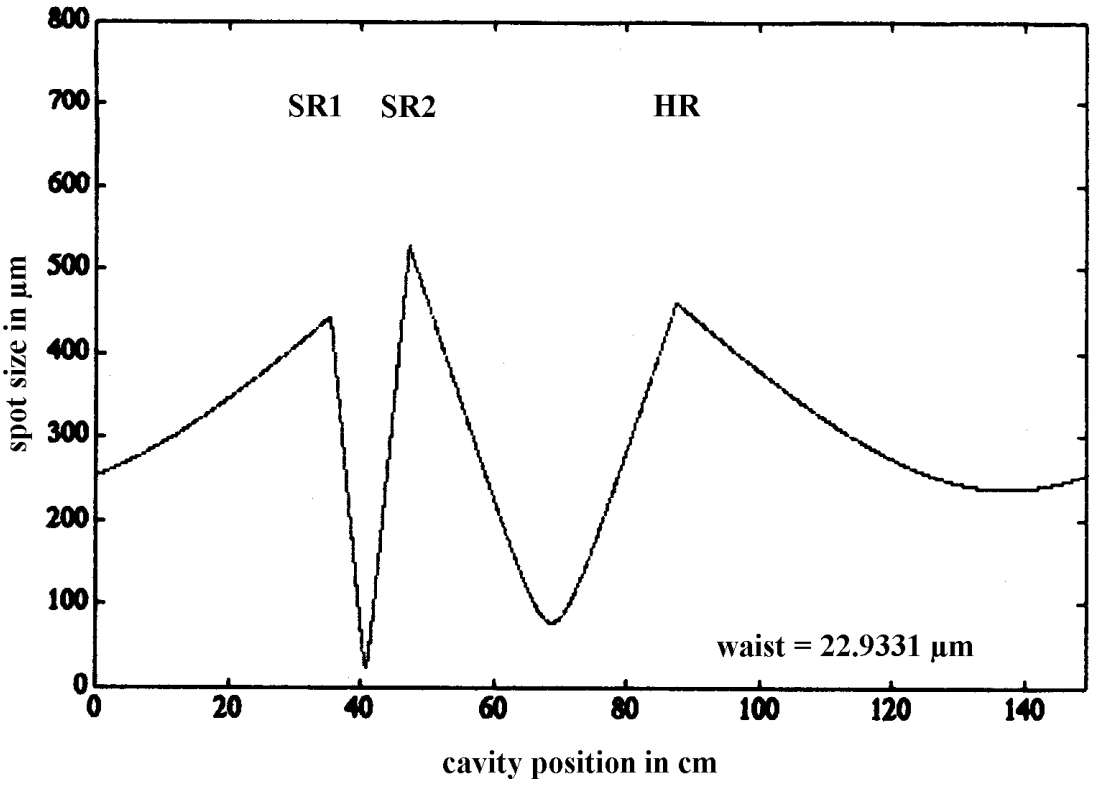

Figure 3.6: Spot size in the cavity

3.3 Optical Elements

In the following sections the basic principles of the optical elements inside the laser cavity are briefly described. All three elements were bought from Coherent Incorporated.

3.3.1 Optical Diode

As discussed in Section 3.1 a disadvantage of standing wave lasers is the occurrence of the spatial hole burning effect. By using a ring cavity this effect is avoided. To force the laser to run unidirectionally in this design, it is necessary to include an element for which lasing in one direction constitutes a big enough loss factor to reduce the gain below the gain threshold. For light traveling in the other direction the element should be essentially lossless [7]. Such an element is called an optical diode. The diode used in this laser consists of an optically active quartz compensation plate and a Faraday rotator (Figure 3.7).

The optically active element is a thin plate of quartz inserted into the beam at Brewster's angle. Its surfaces are cut at Brewster's angle with respect to the optical axis to ensure that the refracted beam inside the crystal propagates along the optical axis. The plane of polarization of the transmitted light will always be rotated in the same direction when viewed in the direction of propagation.

The Faraday rotator consists of a 1.2 cm-long piece of SF-2 glass, also inserted at Brewster's angle. It is surrounded by a magnet which produces a magnetic field in the direction of the refracted beam inside the glass. The

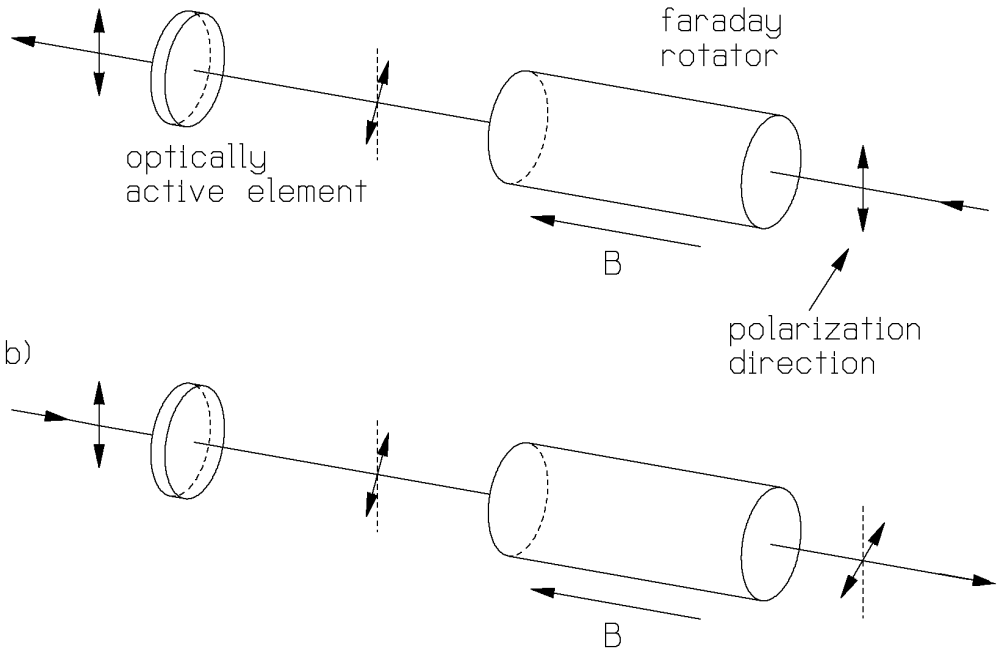

Figure 3.7: Optical diode in (a) forward direction and (b) in backward direction.

rotation of the polarization plane is independent of the direction of propagation. It always has the same direction viewed from the laboratory system.

Because almost all of the elements in the laser cavity are mounted at Brewster's angle the light can be regarded as linearly polarized. In the forward direction, the rotation induced by one element is opposed to that by the second element, while in the backward direction, the two rotations add together. By balancing the magnitudes of rotation a net rotation of 0° can be achieved in the forward direction. The net rotation of a few degrees in the backward direction are enough to induce the desired loss in the cavity by reflection losses at other Brewster surfaces in the cavity.

3.3.2 Birefringent Filter

To obtain a single mode laser, it is necessary to include several mode selective elements. The first selection is made by the birefringent filter. This filter consists of plano-parallel birefringent plates which are mounted in series at Brewster's angle (Figure 3.8). The incident light is assumed to be linearly polarized in the drawing plane of Figure 3.8.

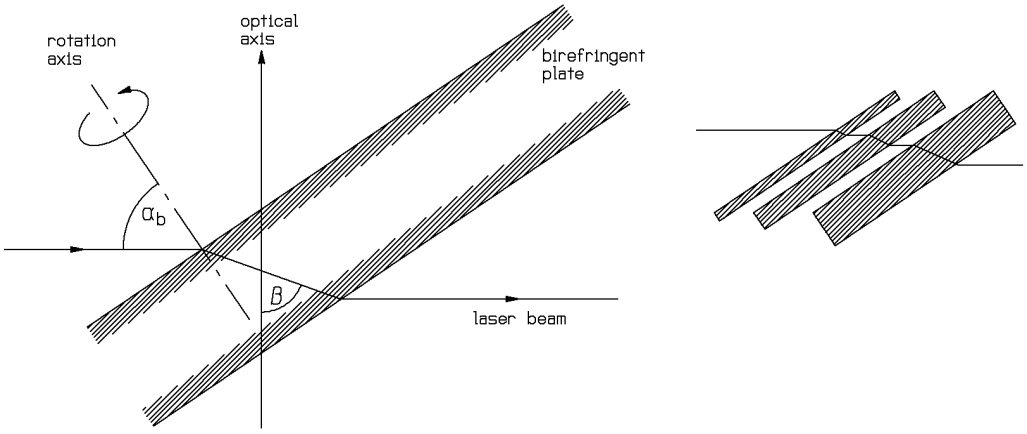

Figure 3.8: Birefringent filter plates

By rotating the plates around the dashed line, the angle β (the angle of the optical axis with respect to the beam through the plate) can be changed without changing the incident angle. This results in a β-dependent polarization of the light after passing each plate. Since the following Brewster surface acts as a weak polarizer the transmission of each plate has a maximum when the emerging light is linearly polarized in the same direction as the incoming light. When the ratio of the thickness of two adjacent plates are integers the peaks

of the transmission curves coincide. The thinnest of the plates determines the free spectral range and the thickest determines the width of the transmission peak. The birefringent filter used had a free spectral range in the order of THz.

3.3.3 Intracavity Assembly

Since the finesse of the birefringent filter is not high enough to select one single mode of the laser cavity, additional elements are necessary. These elements are two etalons combined in the intracavity assembly (ICA).

The thin etalon is a 0.5 mm-thick plate inserted at close-to-normal incidence. The plate is mounted on a galvanometer and can be tilted for frequency adjustment. According to

$$\delta\nu = \frac{c}{2nd} \qquad \text{for} \quad \alpha_{incident} = 0 \tag{3.7}$$

this corresponds to a free spectral range $\delta\nu$ of 200 GHz.

The thick etalon is a 10 mm-thick solid prism-etalon, also inserted at near-normal incidence. The distance d can be varied by scanning the piezo to which it is attached. Equation 3.7 yields a free spectral range of 10 GHz.

Both etalons are coated for approximately 20% reflectivity. This allows a single-mode selection across the entire gain region of the dye.

3.4 Mechanical Considerations

To avoid unnecessary drifts and fluctuations in the optical path-length L the components and their mounts should be as stable as possible. The basic structure for the laser consists of four parallel 1" invar rods. All ele-

ments in the laser are held in place by 1" thick black anodized aluminum plates attached to these invar rods. Invar was chosen because of the small thermal expansion coefficient of $\alpha = 0.9 \cdot 10^{-6} \frac{1}{K}$ [8]. This guarantees rigid connections and minimizes length drifts. In addition to this, the piezo-driven mirrors are glued onto lead-damped mounts to stabilize the mirror motion. The $\frac{1}{4}$"-80 adjusting screws on the mirror mounts are of the highest quality available commercially (from Lees Optical Instrument Company, Inc. in Boulder, Co.). These screws guarantee fine adjustability.

3.5 Dye Pump Station

The flow of the dye solution through the nozzle must be constant to avoid power changes in the output beam and to allow a stable single mode operation. Since the variable pump speed is reasonably stable only at high settings, a regulating bypass valve has to be included in the pump system (Figure 3.9) to be able to run the pump at high speed without exceeding the pressure at the nozzle. The dye solution absorbs heat created by the pump beam and therefore the temperature of the solution rises. A heat exchanger has been built to keep the temperature of the solution constant.

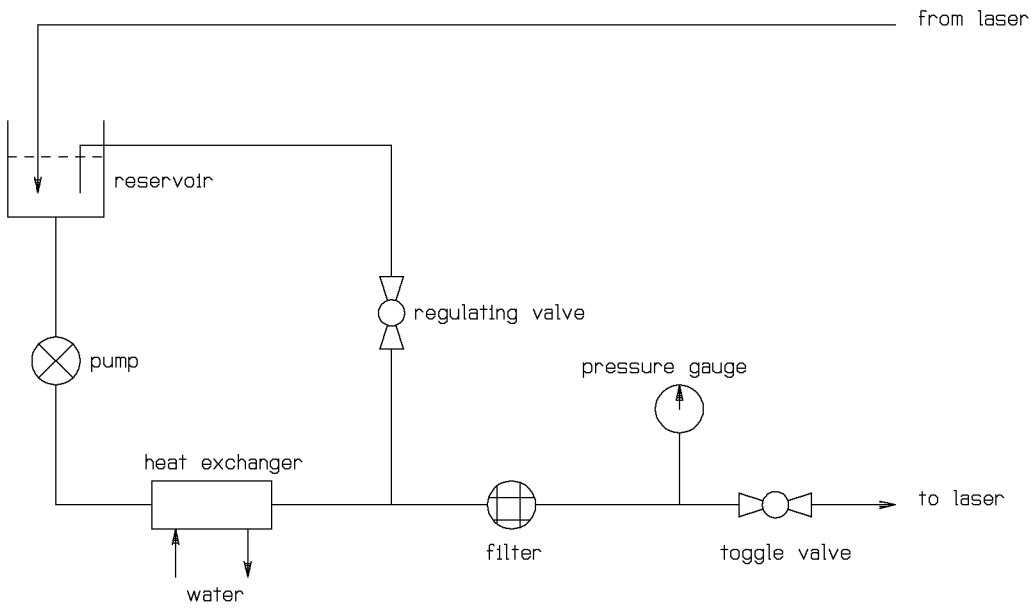

Figure 3.9: Diagram of the dye pump station

Chapter 4

Locking and Stabilization

To obtain a stable single mode laser it is not sufficient to just place the mode selective elements described above into the laser cavity. They also have to be tuned and some of them have to be electronically controlled.

The birefringent filter and the thin etalon have broad enough transmission peaks and large enough free spectral ranges to allow manual adjustment. By using rigid mounting devices and a stable current supply for the thin etalon galvanometer, the drift of the transmission curve over time is negligible. Once these elements are set to yield the desired wavelength, they need not be tuned during normal operation of the laser.

The thick etalon and the cavity itself, as the last mode selective element, each need an electronic feedback loop [9] to avoid mode-hopping of the laser.

4.1 Thick Etalon Lock

The thick etalon lock cannot yield absolute frequency stability since no stable frequency reference is available. It only locks one peak of the etalon transmission curve to the laser wavelength. This lock — and a well adjusted birefringent filter and thin etalon — result in a gain curve which shows only one peak reaching the gain threshold. Since now the transmission maxima of

all the mode selective elements coincide, the highest possible output power can be achieved.

A simplified diagram of the thick etalon lock is shown in Figure 4.1.

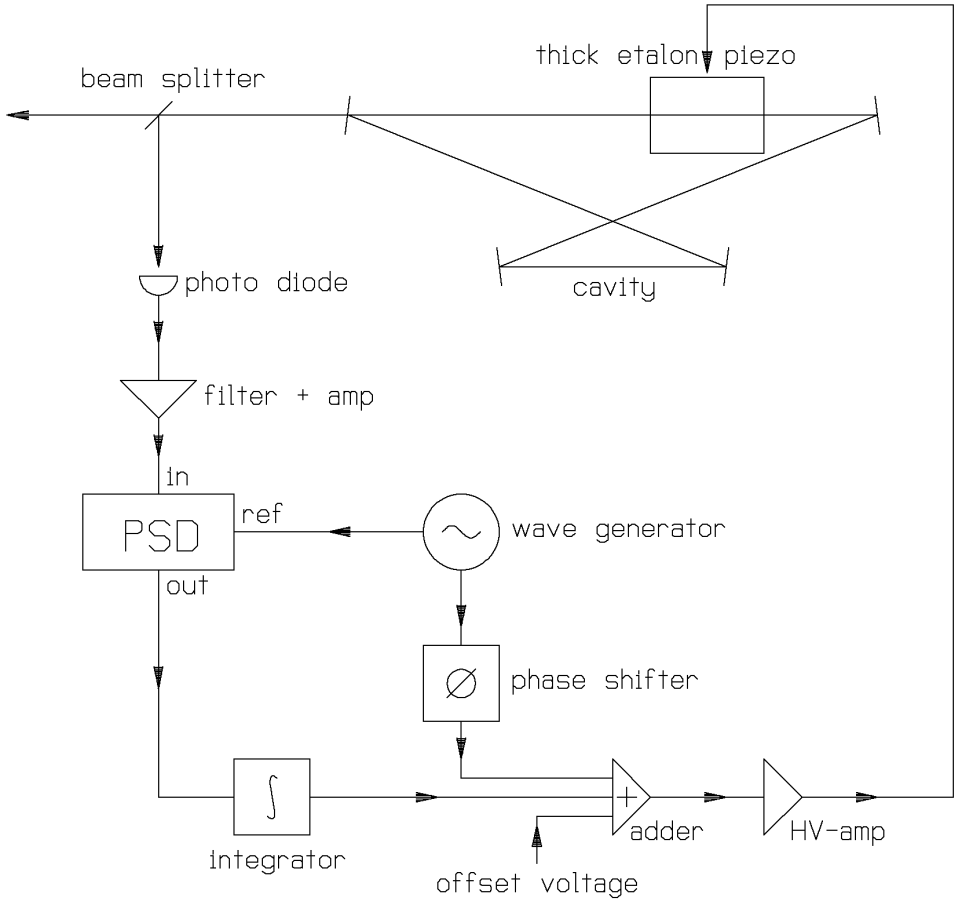

Figure 4.1: Schematic diagram of the thick etalon lock

The principle of operation is illustrated in Figure 4.2. The distance of the reflecting etalon surfaces is modulated by the sinewave generator at

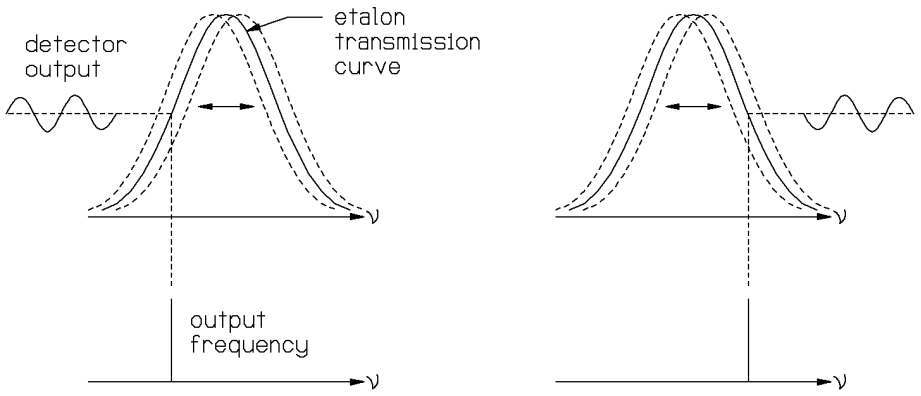

Figure 4.2: Thick etalon response as a function of frequency

1 kHz, and the effect on the output power is monitored by a detector. If the laser frequency drifts to one side of the transmission peak the output power is modulated at the same frequency and with the same phase as the modulation signal. At the peak of the curve, there is no signal at the modulation frequency (but one at twice the frequency). On the other side of the peak the produced output signal and the modulation signal have the same frequency, but are 180° out of phase. With a phase sensitive detector (PSD) this can be converted into an error signal whose amplitude is proportional to the deviation of the transmission peak from the laser frequency and whose sign is dependent on the direction of this deviation. This error signal is added to the modulation signal (and an offset, since the piezos only take voltages of one polarity) and therefore locks the thick etalon by providing negative feedback.

To ensure that the lock-point is the transmission peak and not a point on the side, it is necessary to integrate the error signal, since the piezo bias

position (determined by the offset voltage) almost never corresponds to the maximum of the etalon transmission.

The variable phase shifter can compensate for any phase shifts in the system and gives the possibility to flip the sign of the error signal by shifting the phase by 180°.

Since the thick etalon lock does not directly stabilize or clean up the laser frequency, it does not have to be a very fast lock. The main constraint in any servo loop is that the gain must drop below unity at a cutoff frequency which is lower than any resonance (mechanical or electrical) of the system.

4.2 Locking to an External Cavity

The frequency stabilization is achieved by locking the laser to a very stable reference cavity. This is done using the Hänsch-Couillaud scheme [10]. Figure 4.3 shows a simplified schematic.

A fraction of the linearly polarized laser beam is sent through a confocal reference cavity in a ring configuration. The linear polarizer inside the cavity constitutes a high loss for the component of the incoming light with a polarization plane normal to the transmission axis, so that this component is only reflected at the cavity entrance mirror. The parallel component is not affected by the polarizer and passes through the low loss cavity. It experiences a frequency-dependent phase shift on reflection. The resulting beam therefore shows a frequency-dependent polarization. If the frequency of the incoming light is exactly on resonance, the parallel component is in phase with the normal component and the resulting beam is linearly polarized. Far off resonance

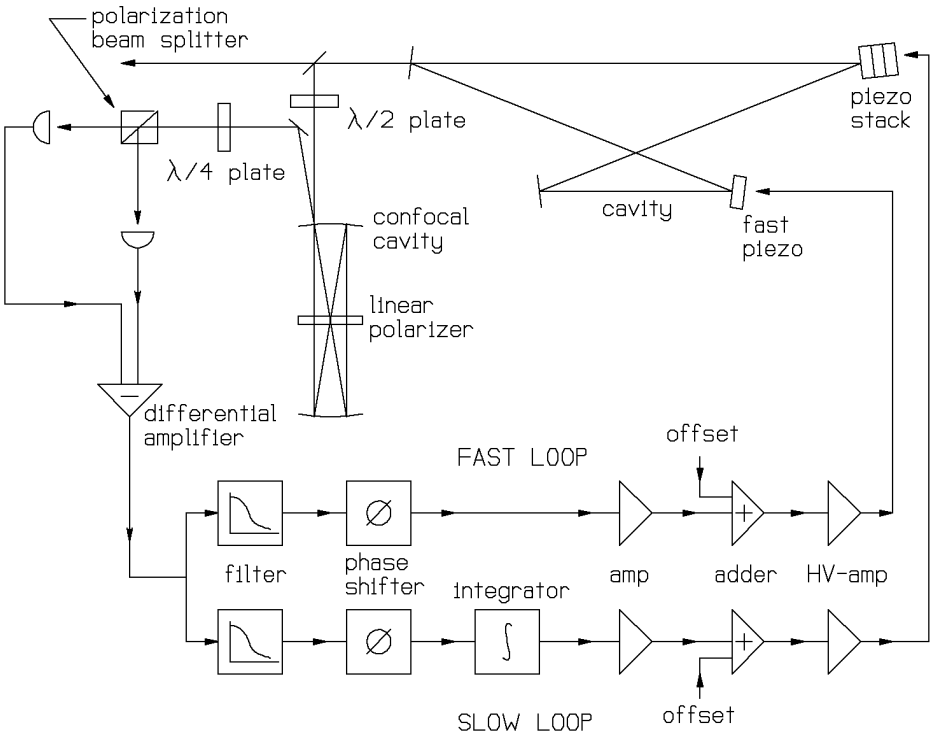

Figure 4.3: Scheme for locking to the external cavity

only the normal component is reflected and so the resulting beam again is linearly polarized. If the frequency is slightly off resonance the phase shift of the parallel component produces elliptically polarized light. The following $\frac{\lambda}{4}$-plate and the polarization beam splitter produce two linearly polarized beams whose difference in intensities is dependent on the ellipticity of the beam reflected by the cavity. The magnitude of this difference signal is determined by the ellipticity, whereas the sign depends on the handedness (the linearly polarized light produced on resonance or far off resonance result in a zero output signal).

The output signal shows the shape of an error signal with far reaching wings and a large slope at the zero-crossing point [10].

The error signal obtained by this scheme is separated into a high and a low frequency component. The high frequency part is amplified and fed back to a single piezo, to which a small cavity mirror is attached. The small mass of the components is necessary to obtain high mechanical resonance frequencies. The electronic filters have to roll off the gain in the loop before the first mechanical resonance is reached. The roll-off frequency in the fast loop is set to about 10 kHz. The slow frequency component is also amplified and fed back to a piezo stack. Since it contains the dc-part of the error signal it has to be integrated to serve as a lock signal. The gain in this part of the loop has to have a roll-off at a much lower frequency since the mechanical resonance frequencies are much lower due to the increased mass of the stack. A piezo stack is necessary to compensate for large drifts of the cavity length by expansion or contraction of several piezos simultaneously.

The wavelength stability of the locked laser depends strongly on the stability of the reference cavity. To avoid strong drifts of the cavity length, the reference cavity is built of invar and will be temperature-stabilized.

This locking scheme offers an easy way to scan the laser frequency. By changing the distance of the mirrors in the reference cavity the resonance frequency changes accordingly. Since the laser is locked to this resonance frequency, the laser follows these changes, as long as the scanning frequency is below all the roll-offs in the lock-loops and as long as the amplitude is small enough for the piezo stack to follow. The varying of the distance is achieved by

scanning the piezos attached to the mirrors in the cavity. The laser has been scanned several hundred MHz with this set-up.

Chapter 5

Results

5.1 Mode Quality

The most obvious way to evaluate the laser is to look at the mode quality of the output beam. The divergence and the spot sizes can be compared with the theoretically expected values from the cavity calculation. The spot sizes have been measured by using a sharp edge to find the points in the beam, where the remaining beam has an intensity of 0.3 and 0.7 times the total intensity. From the distance between these points the actual spot size can be obtained:

position after OC in inches	15	111
spot size in μm	590	1700

Table 5.1: Measured spot sizes

The cavity calculation of the spot size 15" after the output coupler (OC) was approximately 700 μm. The values from Table 5.1 result in an angle of divergence θ of about 0.2 mrad. The measured spot sizes and the angle of divergence of the output beam are smaller than the parameters obtained from the cavity calculation. This is no surprising result, since in the cavity simulation the distances of the mirrors were optimized with respect to the

stability of the cavity whereas the actual cavity was adjusted to produce an output beam which was as clean and tight as possible.

To determine whether the laser runs single mode, the output is monitored with a scanning monitor cavity (see Figure 5.1).

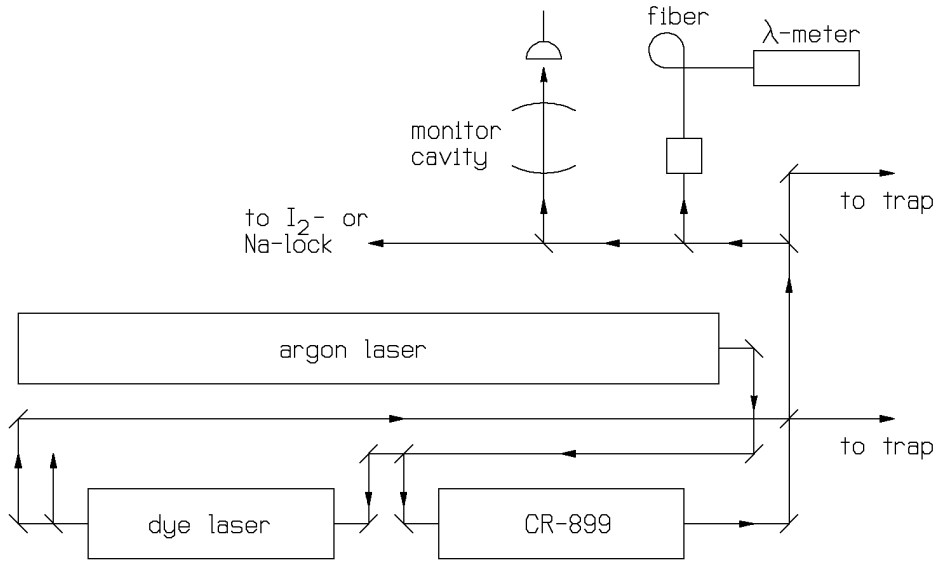

Figure 5.1: Block diagram of the experimental setup

A photograph of the output signal of the cavity and the scan signal is shown in Figure 5.2. It clearly shows a single mode structure.

5.2 Output Power

The output power of the laser was measured with a power-meter which was placed in the beam after the signal for the thick etalon lock and the refer-

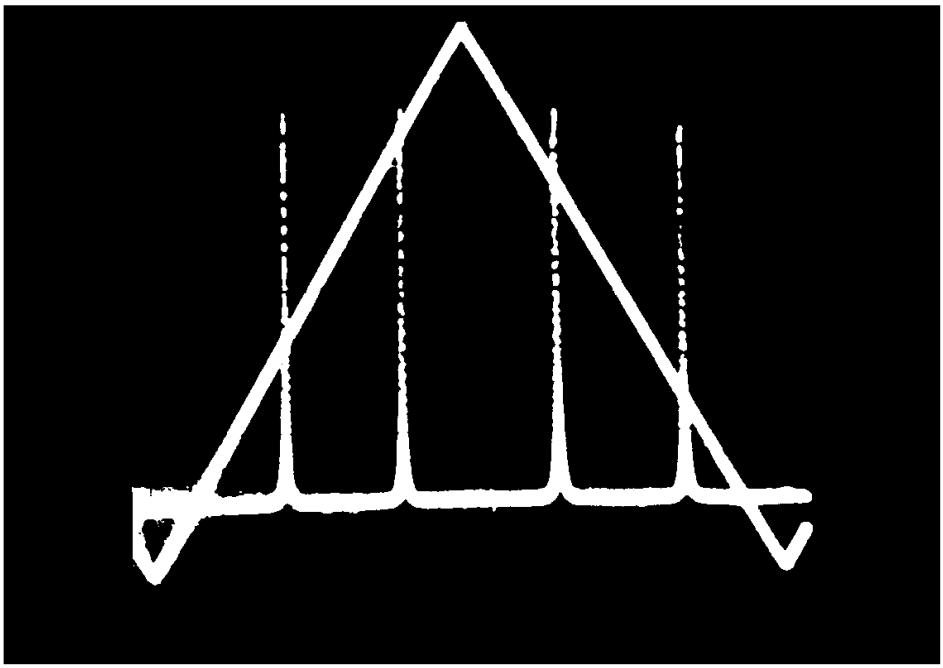

Figure 5.2: Output of the monitor cavity

Two cavity modes are traversed in each scan of the cavity length. Cavity FSR = 1.5 GHz.

ence cavity was split off. The pump power was varied and the output power of the dye laser was measured. Figure 5.3 shows the output power plotted versus the pump power. The pump laser was an argon-ion laser tuned to 514 nm (single line).

During the measurement the thick etalon had to be locked to obtain a stable output power. The measurement was done at a wavelength of 589 nm. The graph in Figure 5.3 does not differ from a typical output power curve for a dye laser.

5.3 Tunability

The required tunability is in the first place limited by the gain curve of the dye. In addition to this, any frequency-dependent loss in the cavity will alter the shape of the tuning curve. To check for eventual unwanted loss factors in the cavity (like wrong coatings on mirrors or other optical devices) the output power at various frequencies was measured and compared with the gain curve of the dye. Figure 5.4 shows the output power versus the wavelength.

As in the previous measurement the thick etalon had to be locked to obtain stable values for the output power. The wavelength was measured with a λ-meter.

The tuning curve shows essentially the characteristics of the dye gain curve (compare with Figure 3.2) and shows no obvious malfunction of any component inside the cavity. Since this measurement was only intended as a test of the components in the cavity, the time-consuming realignment of the cavity for each wavelength has not been made. Also the power-meter was calibrated at 589 nm which possibly lead to inexact measurements at different wavelengths.

5.4 Linewidth

The most important and interesting characteristic of a single mode laser is its linewidth. The linewidth was measured by sending part of the output beam through a high-finesse cavity and measuring the linewidth of the resonance. The cavity was built of two highly reflecting mirrors (50 cm radius of curvature) at a distance of 14". The reflectivity R of both mirrors was

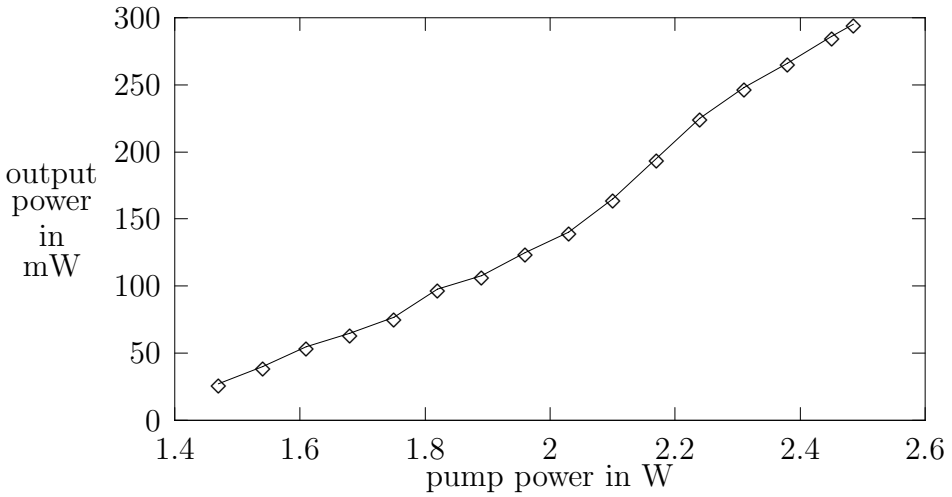

Figure 5.3: Output power curve, single mode

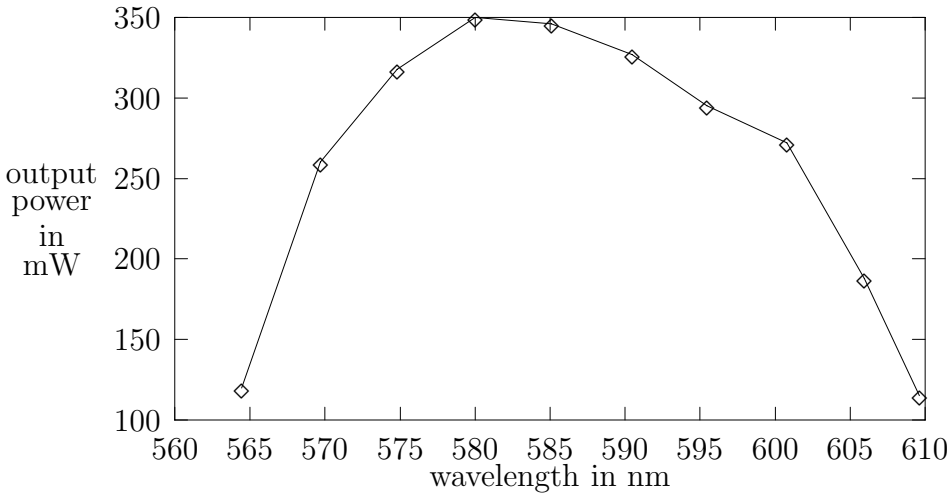

Figure 5.4: Tuning curve, single mode

$R > 99.99\%$. According to

$$F = \frac{\pi\sqrt{R}}{1-R} \tag{5.1}$$

and Equation 3.7 this yields a finesse F of over 30,000 and a free spectral range $\delta\nu$ of 420 MHz. The calculated finesse accounts only for the reflectivity of the mirrors and not for surface roughness, scattering losses, etc. But the theoretical value of 13 kHz for the linewidth of the cavity shows that even when taking these extra losses into account the cavity linewidth is still small compared to a typical linewidth of a dye laser (on the order of a MHz). The linewidth of the light passing through the cavity is measured with an oscilloscope, calibrated by measuring the free spectral range of the cavity and comparing it with the well known theoretical value. This measurement yields a linewidth of 640 kHz. Since the resulting linewidth is caused by a convolution of both lines (laser and cavity) this method can only yield an upper limit for the linewidth of the laser. But due to the high finesse of the test cavity the linewidth is expected to be close to 640 kHz.

5.5 Stability

Due to delays in delivery and machining the temperature stabilization and mounting of the reference cavity on the laser could not be completed in time. Because the reference cavity was not temperature-stabilized by the end of the available time, the drift of the laser frequency over time could not be measured. It depends strongly on the temperature drifts and on the drift of the angle at which the output beam hits the reference cavity (since the length of the ring figure inside the cavity depends on this angle). This angle drift was

especially high since for testing purposes the cavity was mounted on the optical table away from the laser.

Chapter 6

Possible Modifications

6.1 Scanning Brewster Plates

As described in section 4.2 the limit for the scan width of the laser frequency is the piezo stack. It can only be expanded a certain distance without exceeding the voltage limit. The change in the optical pathlength is therefore limited to approximately 2–3 wavelengths. This corresponds to 2–3 free spectral ranges or 400–600 MHz, whereas the reference cavity is able to scan about 4 GHz. To use the whole scan range of the reference cavity, a pair of Brewster plates can be inserted into the laser cavity. These plates are inserted into the beam at Brewster's angle and are mounted on separate galvanometers as illustrated in Figure 6.1. These can be tilted simultaneously, but in opposite

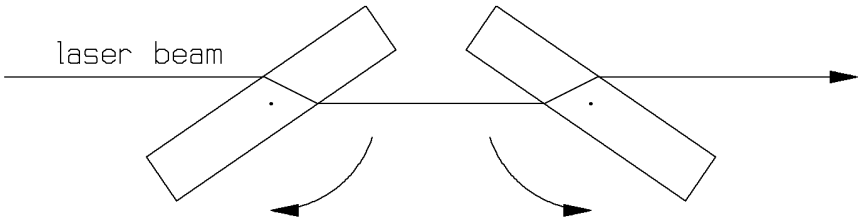

Figure 6.1: Brewster plates

directions, to avoid a steering of the beam. With 1 mm-thick plates a change of 1° of the incident angle results in a change of the optical pathlength which

corresponds to a frequency change of about 4 GHz. The tilting of the galvanometers can be arranged in a feed-forward loop, where the scan signal on the reference cavity piezos is converted into a corresponding current signal to drive the galvanometers. The piezo stack in the laser cavity then only has to correct for small mismatches and would have sufficient dynamic range to lock the laser to the reference cavity resonance as it is being scanned.

6.2 Locking to an Atomic Transition

In case a frequency standard more stable than the temperature stabilized reference cavity is necessary, the laser frequency could be locked to an atomic or molecular transition [11]. This could be done by saturation spectroscopy, which is currently used in the laboratory to lock the commercial CR-899. This technique would offer the advantage that most of the necessary optics (like an electro-optic modulator, cells, etc.) could be used for both dye lasers simultaneously. Only separate electronic devices would have to be used. nly separate electronic devices would have to be used.

BIBLIOGRAPHY

[1] R. Graham, M. Schlautmann, and P. Zoller, Dynamical localization of atomic-beam deflection by a modulated standing light wave, Physical Review A **45**(1) (Jan. 1992).

[2] M. J. Holland, D. F. Walls, and P. Zoller, Quantum nondemolition measurements of photon number by atomic-beam deflection, Physical Review Letters **67**(13) (Sept. 1991).

[3] A. Yariv, *Quantum Electronics*, Wiley, 1988.

[4] T. F. Johnston, Jr., R. H. Brady, and W. Proffitt, Powerful single-frequency ring dye laser spanning the visible spectrum, Applied Optics **21**(13) (July 1982).

[5] W. Demtröder, *Laser Spectroscopy*, Springer-Verlag, 1981.

[6] H. Kogelnik and T. Li, Laser beams and resonators, Applied Optics **5**(10) (Oct. 1966).

[7] T. F. Johnston, Jr. and W. Proffitt, Design and performance of a broad-band optical diode to enforce one-direction traveling-wave operation of a ring laser, IEEE Journal of Quantum Electronics **QE-16**(4) (Apr. 1980).

[8] J. Berber, H. Karcher, and R. Langer, *Physik in Formeln und Tabellen*, Teubner, 1989.

[9] F. M. Gardner, *Phaselock Techniques*, Wiley, 1979.

[10] T. W. Hänsch and B. Couillaud, Laser frequency stabilization by polarization spectroscopy of a reflecting reference cavity, Optics Communication **35**(3) (Oct. 1980).

[11] P. W. Smith, Mode selection in lasers, Proc. IEEE **60** (Apr. 1972).